RESEARCH ARTICLE

American Journal of Botany

Botanical Society of America
leading scientists and educators since 1893

Factors controlling drought resistance in grapevine (*Vitis vinifera*, chardonnay): application of a new microCT method to assess functional embolism resistance

R. Brandon Pratt[1,2], Viridiana Castro[1], Jaycie C. Fickle[1], Angela Madsen[1], and Anna L. Jacobsen[1]

Manuscript received 30 September 2019; revision accepted 15 January 2020.

[1] Department of Biology, California State University-Bakersfield, Bakersfield, CA 93311 USA

[2] Author for correspondence (e-mail: rpratt@csub.edu)

Citation: Pratt, R. B., V. Castro, J. C. Fickle, A. Madsen, and A. L. Jacobsen. 2020. Factors controlling drought resistance in grapevine (*Vitis vinifera*, chardonnay): application of a new microCT method to assess functional embolism resistance. *American Journal of Botany* 107(4): 618–627.

doi:10.1002/ajb2.1450

PREMISE: Quantifying resistance to embolism in woody plants is important for understanding their drought response. Methods to accurately quantify resistance to embolism continue to be debated.

METHODS: We used a new microCT-based approach that quantifies embolized conduits and also analyzes conductive conduits by using an x-ray-dense, iodine-rich tracer that moves though the vascular system and can easily be observed in microCT images. Many previous microCT studies assumed that all conduits were initially conductive, which may not be the case if there are developing or occluded conduits. We compared microCT results to a standard benchtop dehydration method and a centrifuge method. During dehydration, we measured gas exchange and quantified water potential at mortality.

RESULTS: Our microCT curves agreed with previously published microCT curves from the same greenhouse-grown cultivar. We found a significant difference in embolism estimates if we assumed that all water-filled conduits were functional rather than only those containing tracer. Embolism estimates from microCT differed from both the benchtop and centrifuge methods. The benchtop and centrifuge methods did not differ from one another.

CONCLUSIONS: The new microCT method presented here is valuable in sampling species that may contain nonconductive conduits. Disagreement between microCT and two other methods was likely due to differences in the ways they quantify embolism. MicroCT assess the theoretical effect of embolism, whereas benchtop and centrifuge methods directly measure hydraulic conductivity. The theoretical approach does not fully account for the resistances of flow through a complex 3D vascular network.

KEY WORDS active xylem staining; drought; HRCT; hydraulic conductivity; stomata; xylem.

Quantifying plant responses to dehydration is fundamental to understanding adaptations and to predict responses to a drier future. One trait that has received considerable focus is resistance to cavitation and embolism. Cavitation refers to the process by which gas bubbles (emboli) infiltrate conduits and block transport when the negative pressures in the xylem reach a critical threshold (Sperry and Tyree, 1988).

Various methods are used to measure the presence of emboli in vascular systems. One that is increasing in popularity is the use of micro-computer-assisted tomography (microCT; Brodersen and Roddy, 2016; Nolf et al., 2017; Pratt et al., 2020). This method uses x-rays that pass through samples or plants and are sensed by a detector. Samples are rotated and 100s of images are taken and then reconstructed to produce a 3D digital model of a portion of the plant. Structures that are easily observable in microCT images are ones that have sufficient contrast from other structures, with contrast being a function of the x-ray density of a tissue or structure. In plant tissues, the presence of gas is easily resolved because gas has very low x-ray absorption compared to surrounding moist tissues. Advantages of microCT methods are that they provide spatial information about emboli and scans can be done on intact plants leading to reduced chances of certain artifacts.

One thing that could add further interpretive value to the microCT method is if it could be modified to provide unambiguous information on which conduits are functional (Jacobsen and Pratt, 2012; Hacke et al., 2015). It does provide information on which conduits are fluid-filled, but this does not necessarily mean that they are conductive. For instance, developing vessels with fully formed cell walls and containing dilute cytoplasm will appear in microCT images as fluid-filled as will gels in vessels (Jacobsen et al., 2018), yet neither of these are conductive. An abundance of these cells could lead to significant errors and an overestimate of functionality (hydraulic conductivity and embolism resistance; Pratt and Jacobsen, 2018).

A recent method was developed that feeds an iodine-rich compound into the transpiration stream that readily moves through the vascular system. Iodine, being a relatively large element, strongly absorbs x-rays relative to surrounding plant tissues. Using this method, Pratt and Jacobsen (2018) identified which vessels were functional in hydrated plants. In some samples, nonfunctional conduits were relatively numerous (Jacobsen and Pratt, 2012; Pratt and Jacobsen, 2018). The purpose of the present study was to extend this method to dehydrated plants with an aim to understand how plants respond to dehydration and to quantify the hydraulically conductive conduits, those that were fluid-filled but not moving sap, and those that were gas-filled (embolized). This approach, if successful, could significantly improve the microCT method.

Other methods are also commonly used to measure embolism resistance. One is a standard hydraulic method that quantifies the effect of emboli on the hydraulic conductivity of excised samples. Negative pressures are generated in intact plants or large branches dehydrated on a benchtop; thus, this method is sometimes called the benchtop dehydration method. Another method is the standard centrifuge method that uses centrifugal force to generate negative pressures in excised stems or roots (Alder et al., 1997). The hydraulic conductivity of these organs is measured to estimate the presence of emboli and their effect on function over a range of xylem pressures. These data are then used to generate a curve that depicts the resistance to embolism (a vulnerability curve). Later modifications to the original centrifuge method resulted in the development of flow centrifuge techniques, but these modifications may create measurement artifacts (Cochard et al., 2010; Wang et al., 2014; however, see Li et al., 2008). Flow centrifuge methods are not addressed here and were not used in the present study. The two methods that have been suggested as the most reliable are the benchtop dehydration method and the microCT method, and centrifuge-based methods have been criticized by some (Cochard et al., 2015). Here, in addition to working to hone the microCT method, we also compared these three methods because such comparisons have not been commonly made, and there is good evidence that some methods may not agree (Choat et al., 2010; Venturas et al., 2019; Pratt et al., 2020). We also include other physiological and drought-response variables to provide physiological context to vulnerability to embolism data and to evaluate which variables align best with plant function. This context is important because there is no accepted way to produce the "true" vulnerability curve for a species, thus providing additional independent measures of functional responses is valuable for judging the accuracy of any one curve.

In this study, we tested a modified microCT method for measuring vulnerability to embolism that introduced an iodine-rich tracer to mark which vessels were functional in water transport (Pratt and Jacobsen, 2018). We grew grapevine seedlings in a greenhouse and exposed them to a range of water deficits. We fed them iohexol through their roots and imaged them using microCT. We also used benchtop dehydration and a standard centrifuge method and compared the results to those from the microCT method. We measured numerous independent physiological variables that are sensitive indicators of plant performance during drought that were compared to the vulnerability curves.

MATERIALS AND METHODS

One-year-old grapevine (*Vitis vinifera* L., chardonnay, Vitaceae) seedlings were obtained from nursery stock (Willis Orchards, Cartersville, GA, USA) in January 2018. Plants were potted in 3.8-L pots with a well-drained potting soil mix and placed in a glasshouse located on the campus at California State University, Bakersfield, California. Temperature in the greenhouse was set to a maximum of 35°C, and minimum temperature was ambient. After leaf-out, plants were fertilized with a slow-release fertilizer (Osmocote Co., Smart-Release Plant Food Plus, Marysville, OH, USA). Plants were watered twice daily from an overhead watering system, once at 06:00 and again at 13:00 hours, which kept the soil constantly moist to avoid tissue dehydration.

Dehydration experiments

To examine dehydration tolerance, we stopped watering individual plants within the glasshouse (n = 13). Plants were dehydrated one at a time, and the first one was dehydrated on 28 April 2018, and the last one was completed on 19 September 2018. Plants were dehydrated between zero and 12 days to achieve levels of dehydration ranging from fully hydrated to extremely dehydrated. In some cases, if plants were dehydrating very slowly, some moist soil was gently removed from the bottom of the pot to speed drying. Plants ranged in height from 30 to 60 cm, which was important for fitting them into the microCT system described below.

Leaf measurements of dehydrated plants began at 09:00 hours and were taken every 10 min for 60 min. Measurements were made at the leaf level of net carbon assimilation (A_{net}), stomatal conductance (g_s), and chlorophyll fluorescence (quantum efficiency of PSII or ΦPSII) using a gas exchange system (Li-6800 with fluorometer chamber cuvette, Li-Cor, Lincoln, NE, USA). Parameters in the cuvette were kept constant, with photosynthetic photon flux density (PPFD) of actinic light set at 1800 μmol quanta m^{-2} s^{-1}, CO_2 set at 400 ppm (approximately ambient conditions), and the cuvette temperature set to 25°C to buffer temperature changes. Vapor pressure deficit between the leaf and the chamber was adjusted to between 1.5 and 2 kPa to avoid extremes in atmospheric dehydration. The ambient PPFD was between 1500 and 1900 μmol m^{-2} s^{-1}, so 1800 was chosen to avoid light limitation of A_{net}. For each plant (n = 10), one leaf was repeatedly sampled, and each measurement was completed as quickly as possible (measurements took longer in more dehydrated plants). Between measurements, the leaf was removed from the cuvette and exposed to ambient conditions.

In addition to leaf level measurements, water loss and stomatal conductance were measured at the whole-plant level. This was done by sealing the plant pot in plastic wrap to eliminate any water loss from the soil and repeatedly weighing it with an analytical balance (model ED2201-CW, Sartorius, Göttingen, Germany) at each sampling point to measure shoot transpiration.

Additional measurements were made to calculate whole plant conductance. Average leaf temperature was measured with an IR thermometer (Model Fluke 572 CF Infrared Thermometer, Fluke Corporation, Everett, WA, USA). Ambient air temperature and relative humidity (RH) were measured with a datalogger (HOBO MX2301, Onset Corp., Cape Cod, MA, USA). Using these variables, whole plant transpiration (E, mmol m^{-2} s^{-1}) was calculated as E = Water lost/(Leaf area*Time) (Eq. 1). Leaf area was measured using a leaf area meter (Li-3100, Li-Cor). Transpiration was used to calculate whole-plant stomatal conductance (G_s) as $G_s = (E^*P)/VPD$ (Eq. 2). The vapor pressure deficit (VPD) of the leaf was calculated by subtracting the vapor pressure of air in the leaf (calculated using the IR-leaf temperature, assuming RH = 100% inside the leaf) from the vapor pressure of the air, which was calculated using the air temperature and RH (see equations of Campbell and Norman, 1998). Atmospheric pressure (P) was taken as 100 kPa in Bakersfield, CA, USA.

To quantify tissue dehydration, we measured water potential for transpiring leaves (Ψ_l; $n \geq 4$) and for bagged leaves using a pressure chamber (model 2000, PMS Instrument Co., Albany, OR, USA). The bagged leaves were covered with foiled plastic bags that were sealed with zip locks ($n \geq 4$). The whole plant was then placed in a darkened laboratory and allowed to equilibrate for 2 h. This double bagging procedure was done at 10:00 hours after gas exchange measurements. After 2 h, the water potential of the bagged leaves was measured and used to estimate stem xylem pressure potential (P_x). Care was taken to not cut any leaves from the shoot that was to be sampled for embolism, because cuts could introduce air into samples. Instead, leaves from other shoots were sampled.

Shoot conductance (k_{shoot}) was calculated as $k_{shoot} = E/(P_x - \Psi_l)$ (Eq. 3) using whole-plant water loss and the water potential gradient.

Embolism measurements

Embolism of stems, in response to dehydration, was measured using three independent methods. Two methods were applied to the same plants and the same stems ($n = 13$). The first method was a microCT method where stems were imaged to observe the presence of embolized conduits. After P_x was measured, the soil surrounding plant roots was carefully removed and rinsed with water and the root system was kept under water to avoid dehydration. This step took about 10 min. Roots were excised underwater at their tips and put into a vial of 150 mM iohexol (TCI America, Portland, OR, USA). Iohexol was dissolved in deionized water and filtered with a 100 nm pore membrane filter (MAGNA Nylon Supported Plain 0.1 µm, 90 mm GE, Osmonics, New York, NY, USA). Iohexol is an iodine-rich compound that is water soluble and readily taken up into the transpiration stream. The iodine strongly absorbs x-rays; thus, it is a tracer that allows visualization of sap pathways in the plant (Pratt and Jacobsen, 2018). Plants, with their roots in iohexol, were placed in a glasshouse or in a laboratory under light and fans and allowed to transpire for 2 h. This time was effective at getting iohexol into even narrow-diameter conductive vessels (see also Pratt and Jacobsen, 2018). All plants readily transported the iohexol, and it was observed to be present in all plants sampled.

Following the iohexol exposure, intact plants were scanned in a microCT system (Skyscan 2211, Bruker Corp., Billerica, MA, USA). Prior to scanning, all leaves were covered in plastic wrap to prevent transpiration and to make them compact enough to fit into the microCT system. The root system remained submerged in iohexol during the scan. Scans were at a resolution of 3–4 µm. The x-ray settings were 40 kV and 600 µA. Each scan took about 10 min to complete. These scan times are short and energy levels are low, which minimizes the possibility of x-ray damage (Savi et al., 2017). Previous tests have found that these scan settings do not induce visible damage or embolism formation (Venturas et al., 2019; Pratt et al., 2020). Additionally, as further evidence that plants were not damaged, after we fully sampled the plants, the remaining root system and shoot base were replanted, and plants resumed normal growth.

Embolism level was estimated by calculating theoretical conductivity losses. Using the Hagen–Poiseuille relationship and conduit diameters (D), we calculated the theoretical specific conductivity $(\sum(D^4 * \pi))/(128\eta * A) * \rho_{water}$ (kg m^{-1} s^{-1} MPa^{-1}) (Eq. 4), where η is the viscosity of water (0.9544 MPa s); ρ_{water} is the density of water (997.7 kg/m^3), both at 22°C; and A is the stem cross-sectional area (m^2). This temperature was chosen to make K_{ts} comparable to measured hydraulic values (see details below). The presence of embolism was determined as the conduits that were gas-filled (K_{emb}), and the native state functional conduits were analyzed as the ones that contained iohexol tracer (K_{ts}). The maximum conductivity (K_{tmax}) was set equal to $K_{emb} + K_{ts}$. The percentage loss of theoretical hydraulic conductivity (PLC_t) was expressed as $PLC_t = (1 - K_{ts}/K_{tmax})\cdot 100$ (Eq. 5).

After imaging, and after measuring native hydraulic conductivity (described below), the portion of the scanned stem was cut to about 2 cm in air and injected (50 kPa) with compressed and dehydrated gas for about 5 min. The procedure was done to dehydrate the sample. The dry sample was then re-scanned to image all of the vessels in the section (K_{tmax*}). The typical method for calculating PLC_t is to estimate K_{ts} by subtracting the conductivity of embolized conduits from the conductivity of all vessels (i.e., $K_{ts} = K_{tmax*} - K_{emb}$) and to use K_{tmax*} in place of K_{tmax} in Eq. 5, assuming that all the vessels in a dehydrated sample are functional, which may not be the case (Pratt and Jacobsen, 2018). We tested PLC_t calculated using both approaches and predicted that PLC_t calculated using the typical method would underestimate PLC_t due to this assumption.

A second way that embolism was estimated was by using the dehydration method, in which we directly measured hydraulic conductivity of stems (K_s) in their native state. This was done by measuring the same stems imaged for microCT. Stems were carefully cut underwater after they were scanned. The negative pressure in the stems was fully relaxed as the root system had been under water or iohexol for 20–30 min before sampling, which should avoid any cutting artifacts (Trifilò et al., 2014; Venturas et al., 2015). It is possible that refilling of vessels could have occurred; however, this is unlikely because the refilling process in grapevines under tension is slow and the presence of 150 mM iohexol in the sap, which has an osmotic potential of −0.29 MPa (Pratt and Jacobsen, 2018), should have slowed it even further (Knipfer et al., 2016). Moreover, in our microCT images, we did not observe any partially refilled vessels as was seen previously (Knipfer et al., 2016). Initial cuts were made as far away from the portion of the stem for sampling as possible. Cut ends were trimmed with a fresh razor blade. Stem lengths were cut to 15 cm.

Stems were mounted into a tubing apparatus that was connected to an intravenous bag of solution (20 mM KCl, degassed, and filtered with a 100-nm pore filter). Stems were transfused with the solution before the start of the measurements for about 5 min to remove the iohexol solution. The tubing apparatus contained valves that allowed control of the solution through the system. The

bag of solution was elevated to create a pressure head of about 2 kPa at the upstream end of the stem, and the downstream end was connected to a reservoir on an analytical balance (CP124s, Sartorius). The balance was connected to a computer that logged change in mass of solution every 10 s. Before and after pressure-driven flow rates were measured, the flow rate of the solution was measured with no pressure on the stem because stems may be in a nonsteady state due to internal water potentials. The flow rate in the absence of pressure was averaged and subtracted from the pressure-driven flow, and measures were taken when flow rates remained unchanged over a 1-min measurement period. Stems stabilized quickly and most stem conductivity measurements took less than 5 min. Hydraulic conductivity (K_h; kg m s^{-1} MPa^{-1}) was calculated as the corrected pressure-driven flow rate, divided by the pressure head, and multiplied by the stem length. Area specific hydraulic conductivity (K_s) was calculated as K_h divided by stem area.

To express conductivity as a percentage of maximum, stems were flushed with solution at 100 kPa for 1 h to remove emboli, stem ends were trimmed slightly to a final length of 14 cm, and K_h was remeasured. For this species, flushing did not work, and in many cases, the K_h declined, likely due to the formation of gels, which irreversibly occlude conduits and have been described previously for grapevine (Jacobsen and Pratt, 2012). To express K_h as PLC, we took a mean K_h value from stems that were at a P_x close to zero and used this as a maximum K_h (K_{hmax}). For three stems, the K_h was low even though P_x was close to zero. For these stems, the microCT data suggested that there was very little embolism; thus, we set the PLC to the values observed for microCT. PLC was then calculated relatively to the calculated K_{hmax} as $PLC_h = (1 - K_h/K_{hmax})\cdot 100$ (Eq. 6).

A final method used to construct vulnerability curves was to use a standard centrifuge method (Alder et al., 1997; Hacke et al., 2015). This method uses a custom centrifuge rotor in which stems (14 cm long) are mounted and spun to set rotational speeds. The centrifugal force creates negative pressure on the xylem sap at the center of the axis of rotation. Stems were measured for K_h using the tubing apparatus described above before treatment. We did not flush the stems due to the aforementioned problems with clogging by gels. Instead, we started with well-hydrated stems with little or no embolism ($K_{initial}$), which was confirmed with microCT. Stems were then spun in the centrifuge, removed, and K_h was remeasured. This process was repeated at increasing rpms until the K_h was close to zero. The effect of embolism on K_h was expressed as percentage loss of K_h: $PLC_c = (1 - K_h/K_{initial})\cdot 100$ (Eq. 7).

The effect of embolism was also expressed as declines in K_s. Because the stems in this experiment were not flushed, they represented native-state embolism of hydrated plants. For the plants where we had P_x values, we included the initial measurements in our data set of native K_s plotted against water potential.

Vessel length

Vessel length distribution was measured from the stems of nine plants from the same cohort of glasshouse-grown plants. One stem was collected from each hydrated plant for vessel length measures between May and June 2018. Shoots were excised underwater from plants, the ends trimmed with a razor blade, and the proximal end was then fitted with tubing so that a silicone mixture could be injected. Injected segments were selected to be similar in diameter to those used for microCT and hydraulic measures. Silicone injection and vessel length analysis followed the protocol described by Jacobsen et al. (2019) and is consistent with the methods of others (Sperry et al., 2005; Pittermann et al., 2011). Jacobsen et al. (2019) found that this method filled even very small diameter conduits with silicone.

Drought resistance

In April 2018, 12 grapevine plants were planted in the ground in a research plot on the campus of CSUB. The site is an abandoned agriculture field and is currently a protected research and teaching area called the Environmental Studies Area. Plants were watered at the time of planting and watered approximately every other day to keep them moist as they established. Three plants were lost, chiefly due to gopher damage, shortly after planting. The nine remaining plants became established and grew significant shoot tissues during their establishment. Watering was ceased on 8 August 2018 when conditions were hot (>37°C for highs) and dry. By late August, approximately 15 days after watering was stopped, plants began to show signs of stress.

To monitor strain of plants, predawn water potentials began 28 August 2018, when most of the plants were showing some signs of crown dieback. The predawn water potentials were measured on leaves that had been bagged the previous evening with sealed and foiled bags. Just before dawn, leaves in the bags were removed from the plant, placed in a cooler with an ice pack and transported to the laboratory (0.25 km away) for immediate measurement. Measurements continued until plants had 100% shoot dieback.

Another way we monitored strain on the plants was to assess shoot dieback and mortality. Dieback was assessed visually where the shoot was scored on a scale of zero to 100% with zero being no visible shoot damage and 100% being the whole shoot brown and crispy. When plants were at 100% dieback they were recorded as deceased. Mortality was verified by rewatering plants at the end of the experiment and tracking them to see if they resprouted, which none did. Most plants died in early to mid-September 2018 (about 1 month with no water), while two plants survived until late October.

Analyses

Vulnerability curves were fit with a two-parameter Weibull model to calculate the xylem pressures at 10, 50, and 90% loss of conductivity (P10, P50, and P90, respectively). For the dehydration data, a bootstrapping method was used to calculate 95% confidence limits (Hacke et al., 2015; R software 3.5.2, R Foundation for Statistical Computing, Vienna, Austria). The same method was used for the microCT data. For the centrifuge data, we had six different stems for which full vulnerability curves were generated. For these, each curve was fit with a Weibull model, and P10, P50, and P90 were calculated for each stem. These data were used in a 2-way ANOVA that included stem as a random treatment factor and the xylem pressure potential corresponding to 10, 50, and 90% loss of conductivity. This model was run, and 95% confidence limits were generated (JMP 13.2.1, SAS Institute, Cary, NC, USA). Differences among methods for P10, P50, and P90 were determined by assessing overlap between mean values and upper and lower confidence limits. For determining overall difference between methods, a 2-way ANOVA was used with xylem pressure (P10, 50, and 90), and method in the model. Pre-planned

contrasts were used to compare among methods (JMP 13.2.1). This data set was square-root-transformed to meet statistical assumptions. Leaf water potential and P_x were compared using a Pearson correlation analysis. The mean (n = 9) P_x at the point of mortality for field-grown plants was calculated along with the 95% CI.

RESULTS

Grapevine plants were highly sensitive to dehydration. Stomatal conductance declined to about zero at P_x of −0.75 MPa and a Ψ_l of about −1.1 MPa (Fig. 1B). Photosynthesis (A_{net}) followed much the same pattern (Fig. 1D) as did chlorophyll fluorescence (Fig. 1F). Like

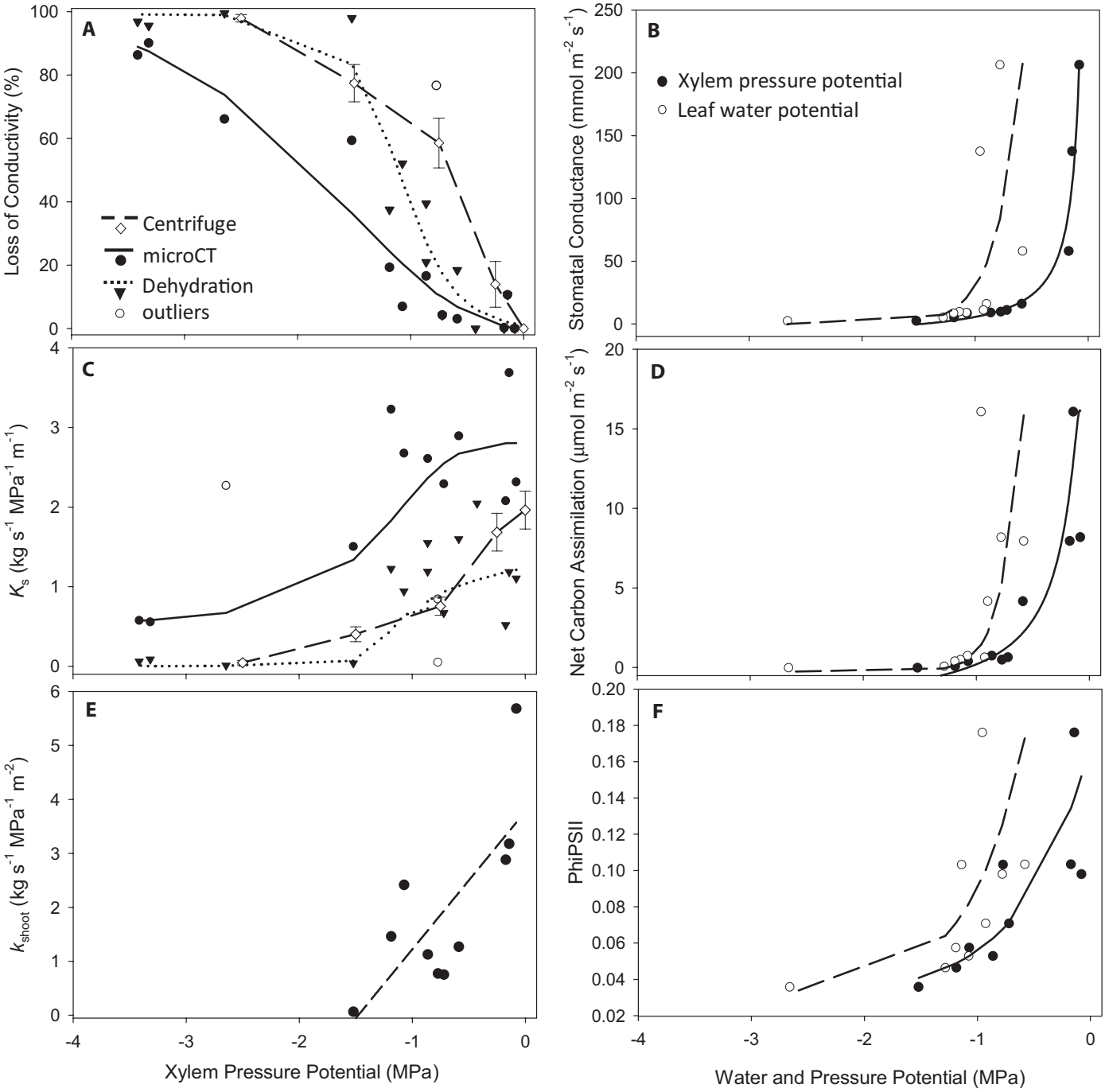

FIGURE 1. Grapevine response to dehydration in glasshouse experiments. Each data point in figures comes from an independent plant, except for the centrifuge vulnerability curves (A, C), which are mean values (n = 6). Vulnerability curves are shown using three different methods, centrifuge, microCT, and dehydration expressed as a percentage loss of hydraulic conductivity (PLC; A) and as xylem specific conductivity (C). Shoot hydraulic conductance is shown in response to declining xylem water potentials (E). The response of leaves is also shown in the form of stomatal conductance (B), net carbon assimilation (D), and chlorophyll fluorescence (F) in response to both xylem pressure potentials and leaf water potential.

g_s, k_{shoot} declined substantially between P_x of zero and −0.75 MPa and was not different from zero by −1.5 MPa (Fig. 1E). We included both P_x and Ψ_l to highlight how they differ. The two variables were significantly and positively correlated (r = 0.825, P = 0.003). As would be expected, Ψ_l was more negative than P_x.

The embolism response indicated that grapevines can avoid substantial embolism only at mild negative pressure. Between P_x of zero and −1.1 MPa, embolism levels were generally less than 20% as seen in microCT images (Figs. 1A, 2A). Likewise K_{ts} did not substantially decline (Fig. 1C). The native K_s data differed and was about 50% PLC at −1.1 MPa. The centrifuge method had little decline in K_s or increase in PLC between zero and −0.25 MPa (Fig. 1A, C); however, PLC sharply increased and K_s decreased between −0.25 and −0.75 MPa (Fig. 1A, C). By P_x = −1.5 MPa, all methods indicated substantial levels of embolism and substantial losses in conductivity (Fig. 1A, C).

Analyzing P10, P50, and P90 across the different methods provides important information in comparing the three methods. The centrifuge had the least negative P10 value, but it differd only from the microCT PLC estimate (Table 1). For P50, the pattern of embolism resistance differed between the methods as follows: microCT PLC > dehydration > centrifuge (Table 1), with the dehydration and centrifuge being marginally different. At P90, there was greater variability, and the only difference was that the microCT was more negative than the dehydration method. Assessing the global difference across the methods, we found that the embolism resistance was greatest for the microCT and was not different between the dehydration and centrifuge methods (Table 1).

Vessels were relatively short in these young stems and provided valuable context for interpreting our results (Table 2). Mean vessel length was 4.19 cm (SD = 1.26 cm, n = 9). The proportion of vessels that were open from the stem end declined rapidly. In 6 of 9 measured stems, there were no vessels that were open to 14 cm, and only 1–4 vessels were open among hundreds in the remaining three samples.

Feeding iohexol into roots to identify conduits that were transporting sap was successful. The iohexol was taken up by the transpiration stream and was clearly visible in the microCT images (Fig. 2). We did detect the presence of nonfunctional vessels (Fig. 2C, arrows). This led to a discrepancy in methods used to calculate PLC_t where the traditional method significantly underestimated PLC_t (Eq. 5; Table 3). The largest

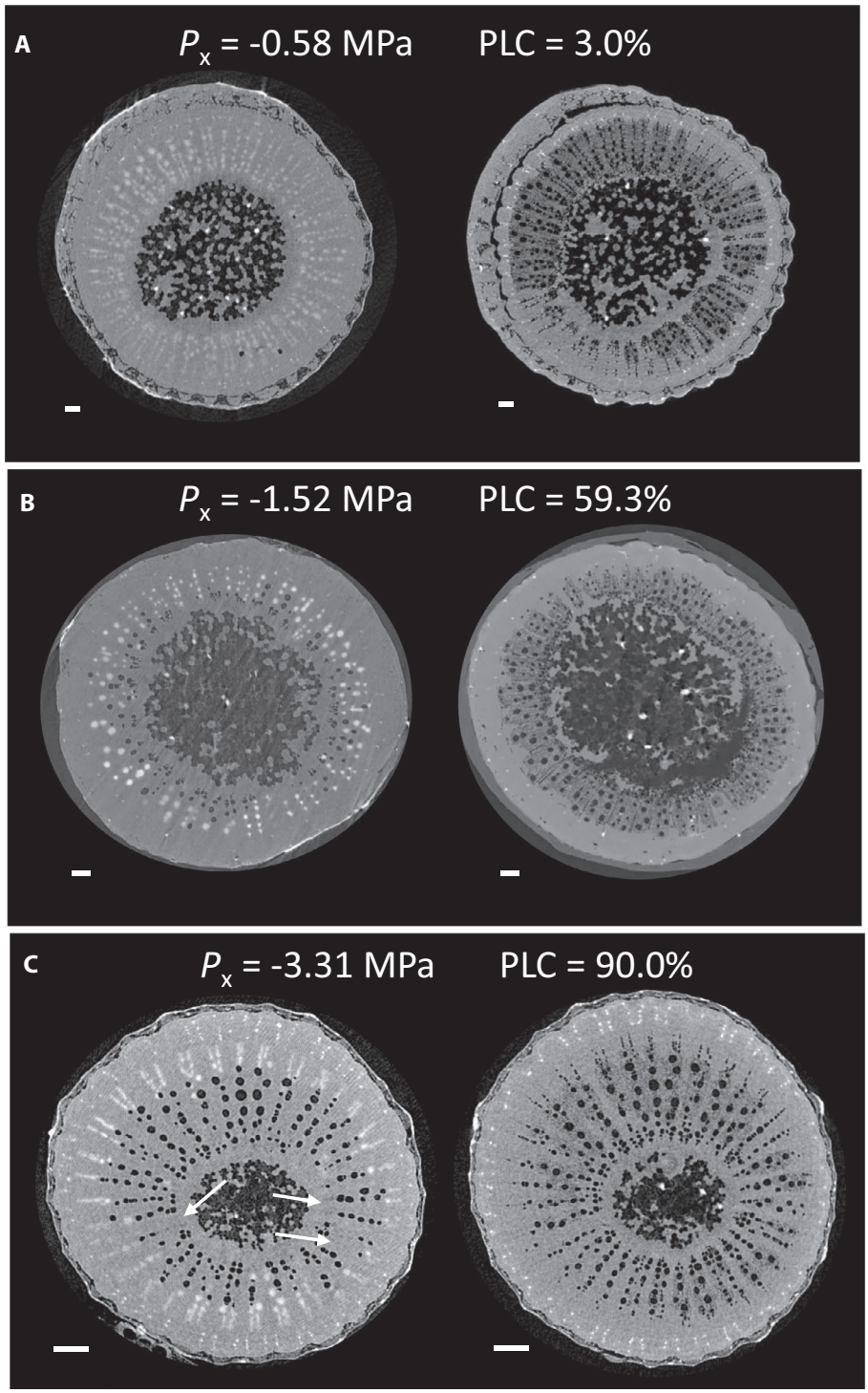

FIGURE 2. Representative images from microCT showing stem xylem at different xylem pressure potentials (P_x). The left image in the different panels is of the intact plant stem, and the white spots in the image represent the presence of iohexol in vessels, whereas black circles are embolized vessels. The panels on the right show the same stem after it has been removed from the plant and dehydrated to observe all the vessels in the tissue. Arrows in panel C point to vessels that are filled with fluid but not transporting iohexol, indicating that they were not functional in transporting water. These same vessels filled with air upon dehydration (right image in C).

TABLE 1. Grapevine resistance to embolism using three different methods and analyzing percentage loss of conductivity.

Method	P10	LCL	UCL	P50	LCL	UCL	P90	LCL	UCL
Dehydration[A]	−0.59[A]	−0.33	−0.77	−1.10[A]	−0.97	−1.24	−1.62[A]	−1.43	−2.59
Centrifuge[A]	−0.24[AB]	0	−0.61	−0.74[A]	−0.37	−1.10	−1.87[AB]	−1.51	−2.24
microCT[B]	−0.72[B]	−0.46	−1.12	−1.89[B]	−1.43	−2.23	−3.49[B]	−1.76	−3.94

Note: LCL and UCL are upper and lower 95% confidence limits. Letters associated with methods denote significant differences.

TABLE 2. Proportion of open vessels in grapevine, including the number of vessels at the silicone injection point and the count of vessels still containing silicone at selected distances from the injection point (n = 9 stems).

Variable	Contained silicone (No.)	Min (no.)	Max (no.)	Open conduits (%)	SD (%)
Injection point (0 cm)	281.67	190	370	100	—
Open to 7 cm	10.90	2	34	4.13	3.74
Open to 14 cm	0.76	0	4	0.29	0.44

TABLE 3. Comparison of two methods to calculate percentage loss of conductivity (PLC_t) from microCT data.

Sample	PLC_t Iohexol[1]	PLC_t Traditional	Delta
1	0.2	0.2	0.0
2	4.2	3.0	1.2
3	76.7	74.4	2.3
4	59.3	52.8	6.5
5	16.6	14.0	2.6
6	19.3	16.9	2.4
7	3.0	1.5	1.5
8	0.0	0.0	0.0
9	6.9	3.6	3.3
10	66.1	66.2	−0.2
11	10.6	11.8	−1.2
12	86.3	88.7	−2.4
13	90.1	80.1	10.0
Mean	33.8	31.8	2.0
	df	***t***	***P***
Paired *t*-test	12	2.1	0.024

Note: See Eq. 5 and discussion of calculation of PLC_t.

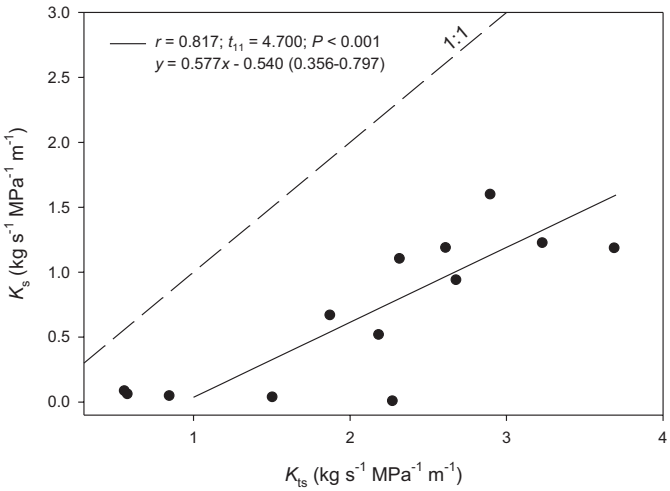

FIGURE 3. Measured stem specific hydraulic conductivity (K_s) compared to the theoretical stem specific hydraulic conductivity (K_{ts}) calculated from microCT images. The slope and 95% confidence limits were calculated using standardized major axis regression and was significantly lower than 1.

discrepancy we observed was 10% (Table 3). When samples were dehydrated by air injection, both conductive and nonconductive vessels filled with air (Fig. 2C).

Both the dehydration and microCT methods generated K_s and K_{ts} values that were significantly correlated (Fig. 3). The K_{ts} values were significantly greater than the K_s values by about 1.7 times. (In Fig. 3, the slope differs significantly from zero.)

Grapevines were planted in a common garden and subjected to drought to determine the P_x at which they started to shed plant parts (dieback) and succumbed to mortality. Dieback in the field began at about –1.44 MPa and rose sharply thereafter (Fig. 4). Mortality of plants (100% dieback) was observed between P_x between −2.68 and −4.04 (mean P_x = −3.20, LCL = −2.82, and UCL = −3.57 MPa; Fig. 4).

Combining data gives insight into factors linked to drought resistance in grapevine. One topic of keen interest is whether embolism is predictive of dieback and mortality. The dieback observed left branches crispy and dead, and we did not observe any resprouting from those branches or any of the plants (i.e., the drought experiment was lethal for all plants). Under mild water deficits, a steep reduction of g_s was the first response of grapevine (Fig. 4). Emboli begin to develop at the P_x (−0.6 MPa) where g_s is very close to the minimum value (Fig. 4). At this P_x, emboli began to rise, reaching about 30% PLC_t and 70% PLC_h at the point of incipient dieback (P_x = −1.3 MPa). Dieback rose sharply at this point, and at about 50% dieback, the PLC_t was also at about 50%, and PLC_h was 90% (Fig. 4). After this point, the dieback proceeded rapidly to 100% (mortality) at P_x = −3.2 MPa. The PLC_t at the point of mortality was just over 80%, whereas the PLC_h was not different from 100%.

DISCUSSION

Comparisons among methods

Some studies have found significant differences in embolism resistance depending on methods used, and grapevine has been of particular interest (Choat et al., 2010; Charrier et al., 2016).

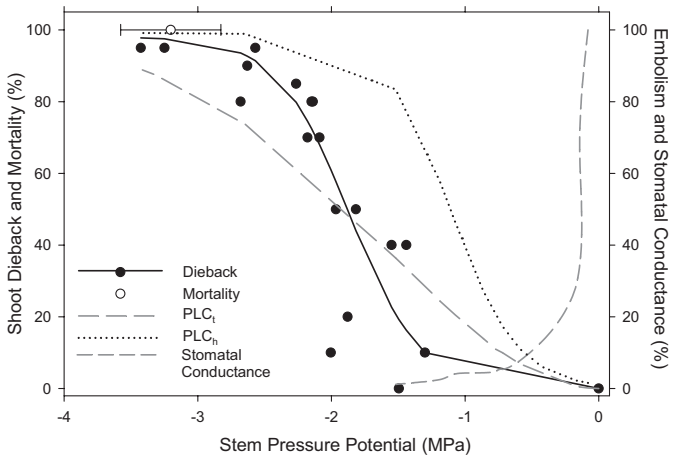

FIGURE 4. Dieback and mortality of field-grown plant in relation to other key variables measured. The mortality data point represents the mean xylem pressure (n = 9) at which plants died and the 95% CI. Each data point for the dieback data represents a different sampling time. Two plants were sampled only once as they suffered 100% dieback after the first sampling and could not be sampled, while other plants were sampled between two and seven times over 2 months.

We found significant differences among microCT and the other methods we used. One hypothesis for this methodological difference has been that the non-invasive microCT method could not distinguish between functional and nonfunctional fluid-filled conduits (Jacobsen and Pratt, 2012; Hacke et al., 2015; Pratt and Jacobsen, 2018). The method that has been commonly used in microCT studies of embolism resistance assumes that all vessels are functional in transporting sap or that all vessels that become air-filled when stems are cut were conductive. In grapevine, fluid-filled nonfunctional conduits could be immature, filled with gels, or contain tyloses. We developed a new microCT method that could distinguish between functional and nonfunctional fluid-filled conduits (Pratt and Jacobsen, 2018) and applied it in this study, for the first time, to examine response to drought. There was a significant difference between the standard microCT analysis and analysis when only functional conduits were included. The standard microCT method overestimated resistance to embolism. The largest difference we observed was a 10% overestimation of embolism resistance. In cases where a species has abundant nonfunctional conduits that are fluid-filled when viewed with microCT, even greater deviation would be expected (Pratt and Jacobsen, 2018).

Some have argued that nonfunctional conduits filled with gels or cytoplasm do not fill with gas upon dehydration (Cochard et al., 2015; Klepsch et al., 2018), which would avoid the error of counting nonfunctional vessels as functional using microCT. Our data suggest that this assumption is not reliable and that nonconductive vessels fill with air upon dehydration (see also Jacobsen et al., 2018 and Pratt and Jacobsen, 2018). Nonconductive conduits may impact both native and maximum conductivity estimates and can thus impact both conductivity and PLC estimates in ways that are not easily corrected.

The microCT method in the present study produced estimates of embolism resistance that were greater than those estimated from native dehydration and the centrifuge methods. Our microCT results agree remarkably well with other microCT-based data (Brodersen et al., 2013; Charrier et al., 2016). This agreement suggests that our findings are generally representative of these different methods and that differences in plant material or precise microCT method cannot account for our results. The high vulnerability to embolism we observed here has been argued to arise due to the presence of long vessels in grapevine and errors that could arise when using the centrifuge method on a long-vesselled species (Choat et al., 2010; Charrier et al., 2016). Two reasons make this "long-vessel artifact" hypothesis unlikely in the present study. First, the young grapevine stems that we sampled did not have particularly long vessels, and the maximum vessel length was shorter than 14 cm for most samples, meaning they would have contained no open vessels. Second, we found that results from the centrifuge method agreed with those of the dehydration method; thus, long-vessel artifacts in the centrifuge cannot explain the high vulnerability of dehydration-based data as we observed for grapevine.

An alternative hypothesis for the discrepancy between microCT and hydraulic methods lies in the way the effect of embolism on conductivity is estimated using the microCT method. All three methods induce negative pressures by either dehydrating the plants intact (microCT and dehydration methods) or by generating negative pressures using centrifugal force. Both the dehydration and centrifuge methods assess the effect of embolism by directly measuring K_h and how it responds to P_x. In contrast, the microCT method estimates K_{ht} from the Hagen–Poiseuille relationship (Eq. 4). This approach assumes that K_h is only dependent on the number of vessels that are sap-filled and their lumen diameters; however, the K_h of the xylem is affected by other resistances that are present as sap flows through the complex 3D xylem pathway including the area and resistance of pits that connect vessels (Jacobsen and Pratt, 2018; Mrad et al., 2018). It appears that as vessels embolize, the decline in K_h outpaces the decline in K_{ht} as has been shown in numerous species (Nolf et al., 2017; Jacobsen et al., 2019; Venturas et al., 2019; Pratt et al., 2020). Previous studies on grapevine have shown that PLC$_t$ never goes above 80% even at −4 MPa (Brodersen et al., 2013; Choat et al., 2010), a P_x past the point of mortality. In other words, the microCT vulnerability to embolism estimates do not agree with the drought-resistance thresholds for grapevine.

Another hypothesis is that cutting stems leads to artifacts (Wheeler et al., 2013). These cutting artifacts have not generally been supported in careful testing (Trifilò et al., 2014; Venturas et al., 2015). Some cutting methods may lead to artifacts, but our methods used here have been carefully and repeatedly tested, and no cutting artifact has been found (Venturas et al., 2015; Pratt et al., 2020).

The centrifuge method and the dehydration method were not significantly different overall. The lack of significant differences between the results with the centrifuge and dehydration methods contrasts with some other studies that find striking differences between the centrifuge method and others (Choat et al., 2010; however, see Jacobsen and Pratt, 2012). The relatively small and insignificant differences we observed between the dehydration and centrifuge vulnerability estimates are likely due to errors associated with repeatedly spinning stems in a centrifuge as has been described previously (Hacke et al., 2015; Tobin et al., 2013).

One challenge with grapevine is that it forms gels that clog stems, making it particularly difficult to remove emboli (Jacobsen and Pratt, 2012). We found that when stems were pressurized

after measuring K_h, their K_h values typically went down after flushing. We have not commonly observed this flushing behavior in woody plants, but we consistently see it in grapevine (Jacobsen and Pratt, 2012; see also Drayton, 2009).

Petioles of grapevines have been found to be quite vulnerable to embolism (Charrier et al., 2016). If the petioles were completely embolized, the P_x estimated with a pressure chamber could be more negative than measured (see also Tobin et al., 2013). There are two reasons we think this is unlikely in this study. First, we commonly imaged petioles along with our stems, and we could see some functional vessels in petioles that were filled with iodine, indicating that they were not fully embolized. Second, this error would have led to artificially high estimates of resistance to cavitation for both the microCT and the dehydration methods. Our dehydration method agreed with the centrifuge method that used centrifugal force to generate a range of P_x values. Also, our microCT vulnerability curve agrees with previous data generated on similar greenhouse-grown material (Brodersen et al., 2013; Charrier et al., 2016).

Tolerance of dehydration in grapevine

We measured a range of physiological variables using methods that are independent of embolism measurements, and these variables are useful in interpreting grapevine drought response and veracity of the vulnerability to embolism measurements. All of our measurements were consistent with grapevines being intolerant of dehydration as others have found (Hochberg et al., 2017). The stomatal response to water deficits appears to be geared to avoid significant emboli for glasshouse-grown plants (Hochberg et al., 2017). After stomata close, stem emboli begin to develop with any additional decline in P_x. Consistent with stomatal closure, net carbon assimilation was near zero by P_x of about −0.75 and Ψ_l of about −1.1 MPa. This result indicates that grapevines can avoid significant embolism via stomatal closure in some cases, which comes at the cost of low levels of carbon assimilation. This condition, if protracted, would require grapevine to draw on carbon stores and would affect production and could lead to increased vulnerability to pests (McDowell et al., 2008). Chlorophyll fluorescence similarly declined in response to both P_x and Ψ_l, indicating substantial photoinhibition at modest water deficits, indicating that chlorophyll fluorescence is highly sensitive to water deficits in a sunny glasshouse and is a sensitive indicator of water stress in grapevines (Flexas et al., 2000). Shoot conductance also showed dramatic declines at mild water deficits. In sum, the data show that grapevine is highly sensitive to slight drops in P_x and Ψ_l, which was confirmed here using multiple independent methodologies.

The embolism and leaf physiological measurements were made on glasshouse-grown plants in containers. We planted some plants into a field plot to examine their drought response. In the field, branches began to die back at P_x of about −1.5 MPa, and most were dead by −3.5 MPa. If the vulnerability curves generated on the glasshouse-grown plants are representative of the field-grown plants (Choat et al., 2010), we can use these curves to understand how embolism relates to dieback and mortality. The shedding of leaves was insufficient to avoid embolism in stems, as all plants kept leaves past the point of embolism and dieback in contrast to the findings of Hochberg et al. (2017). The dieback we observed was fatal, and we did not observe any recovery from dieback, and all plants were killed by the drought treatment. Data from microCT suggested that dieback began at 30%, with complete mortality at about 80% embolism. These values are generally lower than what other studies have observed for dieback and mortality in angiosperms (Davis et al., 2002; Pratt et al., 2008; Kursar et al., 2009; Urli et al., 2013). By contrast, PLC_h indicated that dieback began at about 70% and increased progressively to the point of mortality when embolism was about 100%. One caveat in this analysis is that drought tolerance may have shifted when plants were grown in the field, and we observed that plants wilted (lost turgor) at less negative water potentials in the glasshouse than the field. Seasonal shifts in hydraulics have also been observed in grapevine (Charrier et al., 2018). This is one of the challenges to conducting ecologically realistic experiments using microCT of potted plants.

SUMMARY AND CONCLUSIONS

The chief objective of this study was to use a new microCT method to generate vulnerability to embolism curves that identified which conduits were transporting sap. We were successful in generating such a curve, and our results agreed with previous curves generated using microCT methods. We found a significant difference between PLC estimates using our new method when compared to the traditional microCT method. In cases where large numbers of apparently functional vessels are not conductive, there will be larger deviations. The vulnerability curve produced by the new method did not agree with those generated using a standard dehydration/hydraulic method or a centrifuge method. The microCT method needs further refinement to take into account the xylem anatomical factors that affect hydraulic conductivity beyond Hagen–Poiseuille estimates. Grapevine was confirmed to be highly sensitive to dehydration and to employ a dehydration-avoidance water-use type. Values for the physiological variables we measured were consistent with the vulnerability curves.

ACKNOWLEDGMENTS

Three reviewers are thanked for providing constructive feedback. NSF HRD-1547784 is acknowledged for support. Department of Defense (Army Research Office) proposal No. 68885-EV-REP and contract No. W911NF-16-1-0556 (R.B.P) are gratefully acknowledged.

AUTHOR CONTRIBUTIONS

R.B.P. conceived of the experiment, organized data acquisition, and wrote the initial version of the manuscript. All authors collected data and assisted with analyses. All authors contributed to the text and edited the manuscript.

LITERATURE CITED

Alder, N. N., W. T. Pockman, J. S. Sperry, and S. Nuismer. 1997. Use of centrifugal force in the study of xylem cavitation. *Journal of Experimental Botany* 48: 665–674.

Brodersen, C. R., A. J. McElrone, B. Choat, E. F. Lee, K. A. Shackel, and M. A. Matthews. 2013. In vivo visualizations of drought-induced embolism spread in *Vitis vinifera*. *Plant Physiology* 161: 1820–1829.

Brodersen, C. R., and A. B. Roddy. 2016. New frontiers in the three-dimensional visualization of plant structure and function. *American Journal of Botany* 103: 184–188.

Campbell, G. S., and J. M. Norman. 1998. An introduction to environmental biophysics. Springer Science & Business Media, New York, NY, USA.

Charrier, G., J. M. Torres-Ruiz, E. Badel, R. Burlett, B. Choat, H. Cochard, C. E. Delmas, et al. 2016. Evidence for hydraulic vulnerability segmentation and lack of xylem refilling under tension. *Plant Physiology* 172: 1657–1668.

Charrier, G., S. Delzon, J. C. Domec, L. Zhang, C. E. Delmas, I. Merlin, D. Corso, et al. 2018. Drought will not leave your glass empty: Low risk of hydraulic failure revealed by long-term drought observations in world's top wine regions. *Science Advances* 4: eaao6969.

Choat, B., W. M. Drayton, C. Brodersen, M. A. Matthews, K. A. Shackel, H. Wada, and A. J. McElrone. 2010. Measurement of vulnerability to water stress-induced cavitation in grapevine: a comparison of four techniques applied to a long-vesseled species. *Plant, Cell & Environment* 33: 1502–1512.

Cochard, H., S. Herbette, T. Barigah, E. Badel, M. Ennajeh, and A. Vilagrosa. 2010. Does sample length influence the shape of xylem embolism vulnerability curves? A test with the Cavitron spinning technique. *Plant, Cell & Environment* 33: 1543–1552.

Cochard, H., S. Delzon, and E. Badel. 2015. X-ray microtomography (micro-CT): a reference technology for high-resolution quantification of xylem embolism in trees. *Plant, Cell & Environment* 38: 201–206.

Davis, S. D., F. W. Ewers, J. S. Sperry, K. A. Portwood, M. C. Crocker, and G. C. Adams. 2002. Shoot dieback during prolonged drought in *Ceanothus* (Rhamnaceae) chaparral of California: a possible case of hydraulic failure. *American Journal of Botany* 89: 820–828.

Drayton, W. M. 2009. Embolism and stem hydraulic conductivity in cultivated grapevine. M.S. thesis. University of California–Davis, Davis, CA, USA.

Flexas, J., J. M. Briantais, Z. Cerovic, H. Medrano, and I. Moya. 2000. Steady-state and maximum chlorophyll fluorescence responses to water stress in grapevine leaves: a new remote sensing system. *Remote Sensing of Environment* 73: 283–297.

Hacke, U. G., M. D. Venturas, E. D. MacKinnon, A. L. Jacobsen, J. S. Sperry, and R. B. Pratt. 2015. The standard centrifuge method accurately measures vulnerability curves of long-vesselled olive stems. *New Phytologist* 205: 116–127.

Hochberg, U., C. W. Windt, A. Ponomarenko, Y. J. Zhang, J. Gersony, F. E. Rockwell, and N. M. Holbrook. 2017. Stomatal closure, basal leaf embolism, and shedding protect the hydraulic integrity of grape stems. *Plant Physiology* 174: 764–775.

Jacobsen, A. L., and R. B. Pratt. 2012. No evidence for an open vessel effect in centrifuge-based vulnerability curves of a long-vesselled liana (*Vitis vinifera*). *New Phytologist* 194: 982–990.

Jacobsen, A. L., and R. B. Pratt. 2018. Going with the flow: structural determinants of vascular tissue transport efficiency and safety. *Plant, Cell & Environment* 41: 2715–2717.

Jacobsen, A. L., J. Valdovinos-Ayala, and R. B. Pratt. 2018. Functional lifespans of xylem vessels: development, hydraulic function, and post-function of vessels in several species of woody plants. *American Journal of Botany* 105: 142–150.

Jacobsen, A. L., R. B. Pratt, M. D. Venturas, and U. G. Hacke. 2019. Large volume vessels are vulnerable to water-stress-induced embolism in stems of poplar. *IAWA Journal* 40: 4–22.

Klepsch, M., Y. Zhang, M. M. Kotowska, L. J. Lamarque, M. Nolf, B. Schuldt, J. M. Torres-Ruiz, et al. 2018. Is xylem of angiosperm leaves less resistant to embolism than branches? Insights from microCT, hydraulics, and anatomy. *Journal of Experimental Botany* 69: 5611–5623.

Knipfer, T., I. Cuneo, C. Brodersen, and A. J. McElrone. 2016. In-situ visualization of the dynamics in xylem embolism formation and removal in the absence of root pressure: a study on excised grapevine stems. *Plant Physiology* 171: 1024–1036.

Kursar, T. A., B. M. Engelbrecht, A. Burke, M. T. Tyree, B. E. I. Omari, and J. P. Giraldo. 2009. Tolerance to low leaf water status of tropical tree seedlings is related to drought performance and distribution. *Functional Ecology* 23: 93–102.

Li, Y., J. S. Sperry, H. Taneda, S. E. Bush, and U. G. Hacke. 2008. Evaluation of centrifugal methods for measuring xylem cavitation in conifers, diffuse- and ring-porous angiosperms. *New Phytologist* 177: 558–568.

McDowell, N., W. T. Pockman, C. D. Allen, D. D. Breshears, N. Cobb, T. Kolb, J. Plaut, et al. 2008. Mechanisms of plant survival and mortality during drought: why do some plants survive while others succumb to drought? *New Phytologist* 178: 719–739.

Mrad, A., J. C. Domec, C. W. Huang, F. Lens, and G. Katul. 2018. A network model links wood anatomy to xylem tissue hydraulic behaviour and vulnerability to cavitation. *Plant, Cell & Environment* 41: 2718–2730.

Nolf, M., R. Lopez, J. M. Peters, R. J. Flavel, L. S. Koloadin, I. M. Young, and B. Choat. 2017. Visualization of xylem embolism by X-ray microtomography: a direct test against hydraulic measurements. *New Phytologist* 214: 890–898.

Pittermann, J., E. Limm, C. Rico, and M. A. Christman. 2011. Structure–function constraints of tracheid-based xylem: a comparison of conifers and ferns. *New Phytologist* 192: 449–461.

Pratt, R. B., and A. L. Jacobsen. 2018. Identifying which conduits are moving water in woody plants: a new HRCT-based method. *Tree Physiology* 38: 1200–1212.

Pratt, R. B., A. L. Jacobsen, R. Mohla, F. W. Ewers, and S. D. Davis. 2008. Linkage between water stress tolerance and life history type in seedlings of nine chaparral species (Rhamnaceae). *Journal of Ecology* 96: 1252–1265.

Pratt, R. B., V. Castro, J. C. Fickle, and A. L. Jacobsen. 2020. Embolism resistance of different aged stems of a California oak species (*Quercus douglasii*): Optical and microCT methods differ from the benchtop-dehydration standard. *Tree Physiology* 40: 5–18.

Savi, T., A. Miotto, F. Petruzzellis, A. Losso, S. Pacilè, G. Tromba, S. Mayr, and A. Nardini. 2017. Drought-induced embolism in stems of sunflower: a comparison of in vivo micro-CT observations and destructive hydraulic measurements. *Plant Physiology and Biochemistry* 120: 24–29.

Sperry, J. S., and M. T. Tyree. 1988. Mechanism of water stress-induced xylem embolism. *Plant Physiology* 88: 581–587.

Sperry, J. S., U. G. Hacke, and J. K. Wheeler. 2005. Comparative analysis of end wall resistivity in xylem conduits. *Plant, Cell & Environment* 28: 456–465.

Tobin, M. F., R. B. Pratt, A. L. Jacobsen, and M. E. De Guzman. 2013. Xylem vulnerability to cavitation can be accurately characterised in species with long vessels using a centrifuge method. *Plant Biology* 15: 496–504.

Trifilò, P., F. Raimondo, M. A. Lo Gullo, P. M. Barbera, S. Salleo, and A. Nardini. 2014. Relax and refill: xylem rehydration prior to hydraulic measurements favours embolism repair in stems and generates artificially low PLC values. *Plant, Cell & Environment* 37: 2491–2499.

Urli, M., A. J. Porté, H. Cochard, Y. Guengant, R. Burlett, and S. Delzon. 2013. Xylem embolism threshold for catastrophic hydraulic failure in angiosperm trees. *Tree Physiology* 33: 672–683.

Venturas, M. D., E. D. MacKinnon, A. L. Jacobsen, and R. B. Pratt. 2015. Excising stem samples underwater at native tension does not induce xylem cavitation. *Plant, Cell & Environment* 38: 1060–1068.

Venturas, M. D., R. B. Pratt, A. L. Jacobsen, V. Castro, J. C. Fickle, and U. G. Hacke. 2019. Direct comparison of four methods to construct xylem vulnerability curves: differences among techniques are linked to vessel network characteristics. *Plant, Cell & Environment* 42: 2422–2436.

Wang, R., L. Zhang, S. Zhang, J. Cai, and M. T. Tyree. 2014. Water relations of *Robinia pseudoacacia* L.: Do vessels cavitate and refill diurnally or are R-shaped curves invalid in *Robinia*? *Plant, Cell & Environment* 37: 2667–2678.

Wheeler, J. K., B. A. Huggett, A. N. Tofte, F. E. Rockwell, and N. M. Holbrook. 2013. Cutting xylem under tension or super-saturated with gas can generate PLC and the appearance of rapid recovery from embolism. *Plant, Cell & Environment* 36: 1938–1949.